Microscopic description of elastic and inelastic proton scattering from ^{208}Pb

M. Dupuis, S. Karataglidis, E. Bauge, J.-P. Delaroche, and D. Gogny

Commissariat à l'Energie Atomique,
Département de Physique Théorique at Appliquée,
Service de Physique Nucléaire, BP 12, 91680 Bruyères-le-Châtel, France

(Dated: February 9, 2008)

Abstract

Information on the equation of state (EOS) of neutron matter may be gained from studies of ^{208}Pb. Descriptions of ^{208}Pb require credible models of structure, taking particular note also of the spectrum. Such may be tested by analyses of scattering data. Herein, we report on such analyses using an RPA model for ^{208}Pb in a folding model of the scattering. No *a posteriori* adjustment of parameters are needed to obtain excellent agreement with data. From those analyses, the skin thickness of ^{208}Pb is constrained to lie in the range $0.13 - 0.17$ fm.

PACS numbers: 21.60.Jz,24.10.Ht,24.10.Eq

Interest in large-scale nuclear structure models for ^{208}Pb, and the specification of matter densities therefrom, is topical [1, 2]. The neutron skin thickness ($S = \sqrt{\langle r_n^2 \rangle} - \sqrt{\langle r_p^2 \rangle}$) of a heavy nucleus is related to the radius of a neutron star [3], by virtue of the equation of state of neutron matter, and understanding this relationship requires detailed knowledge of the requisite proton and neutron densities, for which ^{208}Pb has been used as the example. There is a proposal to measure the skin thickness by parity-violating electron scattering from ^{208}Pb at the Jefferson Laboratory [4]. Thus realistic nuclear structure models are required in order to understand neutron densities in heavy nuclei as well as neutron matter.

Previous estimates of the skin thickness of ^{208}Pb, based on analyses of available electron and nucleon scattering data, range from 0.1 to 0.3 fm [2, 5]. But the skin thickness alone is not a sufficient constraint on the models of structure [2], and a proper evaluation of the neutron density requires analyses of scattering data, for which proton scattering data from ^{208}Pb are particularly suited. The dominance of the isoscalar $^3S_1$ component of the nucleon-nucleon (NN) interaction [6] ensures that proton scattering probes the neutron density and vice-versa. Elastic scattering probes the neutron density directly; inelastic scattering from ^{208}Pb probes the transitions within the neutron surface and may provide additional information by which the skin thickness and neutron EOS may be further constrained. It is the purpose of this letter to use the Random Phase Approximation (RPA) to obtain the spectrum of ^{208}Pb and to evaluate the wave functions obtained therefrom in analyses of elastic and inelastic proton scattering data. Such provides sensitive constraints to the neutron density in ^{208}Pb.

Microscopic optical potentials based on the Melbourne g folding model [2, 6, 7, 8] have been successfully used in describing intermediate energy nucleon-nucleus (NA) elastic scattering without any *a posteriori* adjustment of parameters. Therein, the optical potential for elastic scattering is obtained from the folding of the NN g matrices for infinite matter with the density matrix of the ground state of the target nucleus. However, the reliability of those optical potentials so obtained rests upon the specification of a credible model of structure for the target. As the optical potentials are found from the folding of effective NN interactions, which are one-body operators with respect to the target nucleons, a requirement is that the chosen model of structure exhibits nucleon degrees of freedom. Excellent agreement with data has been achieved in the analyses of elastic scattering of 65 and 200 MeV data across the mass range [6] and of exotic nuclei from hydrogen [7, 9]. In the case of ^{208}Pb, analyses of elastic scattering data allowed discrimination between disparate models of ^{208}Pb which, while predicting the same skin thickness, predicted different matter densities which were reflected in the calculated cross sections [2].

Excellent agreement also has been achieved in describing inelastic scattering in light nuclei self-consistently when using the same effective g matrix as the transition operator within a distorted wave approximation (DWA) for the scattering, and when the transition density matrix elements are obtained from the same underlying structure models. This has been illustrated only for light nuclei [6]. Of particular note is the case of ^{6}He [6, 7]: the neutron halo in ^{6}He was unambiguously established only with a self-consistent analysis of elastic and inelastic scattering data.

With the RPA it is possible to describe inelastic scattering from heavy nuclei with the same level of agreement as that for scattering from light nuclei. This allows for evaluation of the models of nuclear structure for heavy nuclei, for which the specification of excited states and of transitions to them is possible, providing additional constraints to the neutron density. Using the RPA and quasi-particle RPA (QRPA) models for heavy nuclei to obtain

density matrices is akin to the use of no-core shell models for light nuclei. Herein, we shall use the Melbourne g folding model to obtain microscopic optical potentials for use in scattering analyses and thus evaluate the wave functions obtained from the RPA.

The microscopic g-folding optical potential for NA elastic scattering has been described in detail in a review article [6]; we present a brief summary of the model illustrating the salient points with regards to the nuclear structure.

The microscopic, nonlocal, optical potential is obtained from the effective NN g matrices in infinite matter. NN g matrices for infinite matter are solutions of the Bruckner-Bethe-Goldstone equation in momentum space [6], and are derived from the Bonn-B potential [10] for the calculations presented herein. We obtain effective NN g matrices in coordinate space for finite nuclei whose Fourier transforms best map those momentum space (infinite nuclear matter) values. The effective g matrices so obtained, which contain central, tensor, and two-body spin-orbit terms, are folded with the ground state density matrix elements, obtained from the assumed model of structure, to give the optical potential for elastic scattering. The optical potential so defined is complex, energy-dependent and nonlocal. It has the form [6]

$$\begin{aligned} U(\mathbf{r},\mathbf{r}';E) = \delta\left(\mathbf{r}-\mathbf{r}'\right) & \\ \sum_{\alpha_1 m_1 \alpha_2 m_2} \rho_{\alpha_1 m_1 \alpha_2 m_2} \int \varphi^*_{\alpha_1 m_1}(\mathbf{s}) g_D(\mathbf{r},\mathbf{s};E) \varphi_{\alpha_2 m_2}(\mathbf{s})\, d\mathbf{s} & \\ + \sum_{\alpha_1 m_1 \alpha_2 m_2} \rho_{\alpha_1 m_1 \alpha_2 m_2} \varphi^*_{\alpha_1 m_1}(\mathbf{r}) g_E(\mathbf{r},\mathbf{r}';E) \varphi_{\alpha_2 m_2}(\mathbf{r}') & \\ = U_D(\mathbf{r};E)\delta\left(\mathbf{r}-\mathbf{r}'\right) + U_E(\mathbf{r},\mathbf{r}';E)\ , & \quad (1) \end{aligned}$$

where the subscripts D, E designate the direct and exchange contributions, respectively, $\alpha \equiv \{n,l,j\}$, corresponding to the occupied single-particle orbits, and

$$\rho_{\alpha_1 m_1 \alpha_2 m_2} = \left\langle \Psi_{J_i M_i} \left| a^\dagger_{\alpha_1 m_1} a_{\alpha_2 m_2} \right| \Psi_{J_i M_i} \right\rangle\ , \qquad (2)$$

is the density matrix. (For ^{208}Pb, $J_i = M_i = 0$.) The coordinates $\mathbf{r}$ and $\mathbf{r}'$ are projectile coordinates. The coordinate-space code DWBA98 [11] has been used to obtain the results presented herein.

Inelastic scattering is obtained in the DWA using the effective g matrices, specified for elastic scattering, as the transition operators. The DWA transition amplitudes can be written as

$$\begin{aligned} T^{M_f M_i \nu' \nu}_{J_f J_i}(\theta) = \left\langle \chi^{(-)}_{\nu'}(\mathbf{k_o}0) \right| \left\langle \Psi_{J_f M_f}(1\cdots A) \right| A\mathbf{g}_{\rm eff}(0,1) & \\ \mathcal{A}_{01} \left\{ \left| \chi^{(+)}_{\nu}(\mathbf{k}_i 0) \right\rangle \left| \Psi_{J_i M_i}(1\cdots A) \right\rangle \right\}\ , & \quad (3) \end{aligned}$$

where the distorted wave functions are denoted by $\chi^{(\pm)}_\mu(\mathbf{k}q)$ for an incoming/outgoing proton with spin projection μ, wave vector $\mathbf{k}$ and coordinate set 'q' (either 0 or 1). The nuclear wave functions are denoted by $\Psi_{JM}(1\cdots A)$ and, since all pairwise interactions between the projectile and every target nucleon are assumed to be the same, it is convenient to make a cofactor expansion of the nuclear wave functions from which the transition amplitudes

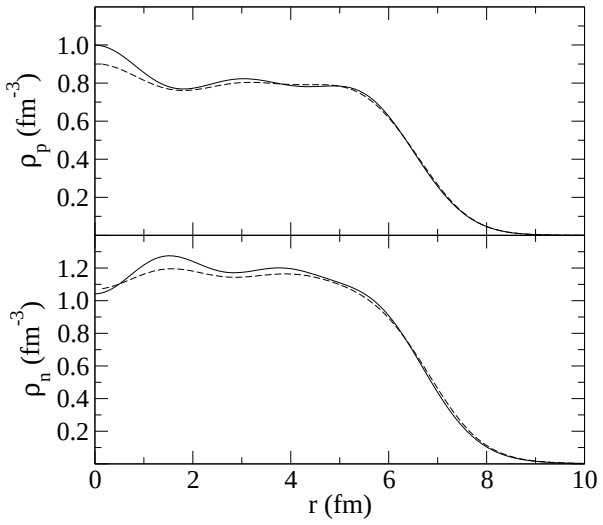

FIG. 1: Proton (top) and neutron (bottom) densities for ^{208}Pb. The results obtained from the RPA and SkM* models are shown by the solid and dashed lines, respectively.

expand to the form, for spin-zero targets,

$$T^{M_f M_i \nu' \nu}_{J_f J_i}(\theta) = \sum_{\alpha_1 \alpha_2 m_1 m_2} \frac{(-1)^{j_1 - m_1}}{\sqrt{2J_f + 1}} \langle j_2\, m_2\, j_1\ -m_1 |\, J_f\, M_f \rangle \left\langle J_f \left\| \left[a^\dagger_{j_2} \times \tilde{a}_{j_1} \right]^{J_f} \right\| 0 \right\rangle \times \left\langle \chi^{(-)}_{\nu'}(\mathbf{k}_o 0) \right| \langle \varphi_{\alpha_2 m_2}(1) |\, \mathbf{g}_{\rm eff}(0,1) \mathcal{A}_{01} \left\{ \left| \chi^{(+)}_{\nu}(\mathbf{k}_i 0) \right\rangle | \varphi_{\alpha_1 m_1}(1) \rangle \right\} . \quad (4)$$

The one-body transition density matrix elements are obtained from the relevant structure model. Exchange terms enter naturally by the action of the two-body antisymmetrisation operator A_{01} on the bound nucleon and projectile in the initial state. The optical potentials and observables obtained therefrom are also calculated using DWBA98 [11].

The densities for the ground state of and transitions in ^{208}Pb were obtained from an RPA calculation using the D1S effective NN force of Gogny [12, 13], which is density dependent and includes finite-range exchange terms. That is used in a self-consistent RPA theory to obtain the relevant density matrix elements and single-particle wave functions. The RPA accounts for ground state correlations induced by collective excitations, beyond the Hartree-Fock approximation, and allows for the specification of transitions to excited states. For comparison in elastic scattering, we have also used densities obtained from a Skyrme-Hartree-Fock calculation using the SkM* interaction [14]. That model was deemed most appropriate for the description of the ground state of ^{208}Pb based on analyses of the neutron skin thickness, elastic electron scattering data and elastic proton and neutron scattering data [2]. The predicted skin thickness from the SkM* model is 0.17 fm [2] while that from our RPA calculation is 0.13 fm.

The densities, from the RPA and SkM* models of structure, and normalised to proton and neutron number, are shown in Fig. 1. The results obtained from the RPA and SkM* models for both the proton and neutron densities largely agree with each other. The predicted

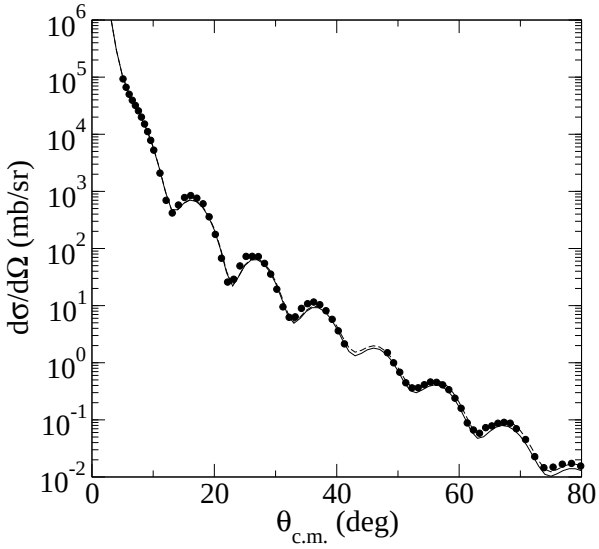

FIG. 2: Elastic scattering of 121 MeV protons from ^{208}Pb. The data of Nadasen *et al.* [15] are compared to the results of g-folding optical model calculations made using SkM* (solid line) and RPA (dashed line) densities.

proton rms radii are 5.47 fm and 5.45 fm for the RPA and SkM* models, respectively, while the predicted neutron rms radii are 5.59 fm and 5.62 fm, respectively. This significant difference in the neutron radii is reflected in the neutron density only at the surface, where the RPA model predicts a sharper surface leading to the smaller skin thickness.

As there are no available elastic scattering data at 135 MeV, the energy at which relevant inelastic scattering data exist, we compare results of the g-folding optical model calculations for the scattering using the RPA and SkM* densities with data taken at 121 MeV [15]. Those comparisons are shown in Fig. 2. Note that these calculations are predictive: no adjustments at all have been made to find a better fit to the data. Clearly, there is excellent agreement between the results of the calculations and the data indicating that the densities obtained from both the RPA and SkM* models are reliable. The cross section is insensitive to the difference in the models which is largely confined only to the surface. This is expected as the optical potential is dependent on the volume integral of the density and so surface effects are relatively minor. Hence, to investigate the surface we turn to inelastic scattering. However, we only use the RPA in those analyses as the Skyrme-Hartree-Fock models cannot specify transitions.

As a first test of the transition densities obtained from the RPA for the transitions to the 2^+_1 (4.08 MeV) and 3^-_1 (2.61 MeV) states in ^{208}Pb, we calculate the B($E2$) and B($E3$) values for those transitions. The values obtained from our model are 0.296 e^2fm^4 and 0.692 e^2fm^6 for the B($E2$) and B($E3$) respectively. Those values obtained from experiment are 0.318(13) e^2fm^4 [16] and 0.611(12) e^2fm^6 [17] for the B($E2$) and B($E3$), respectively. The excellent level of agreement between our model results and the data indicates that no effective charges are needed in the transition matrix elements to correct for any truncations in the model space. Therefore, we may use the bare transitions density matrix elements in the calculations of inelastic scattering without the use of effective charge corrections.

The Melbourne g matrix at 135 MeV has been used successfully in analyses of scattering from ^{3}He and ^{12}C [6]. We have used that g matrix in the calculations of the DWA transition

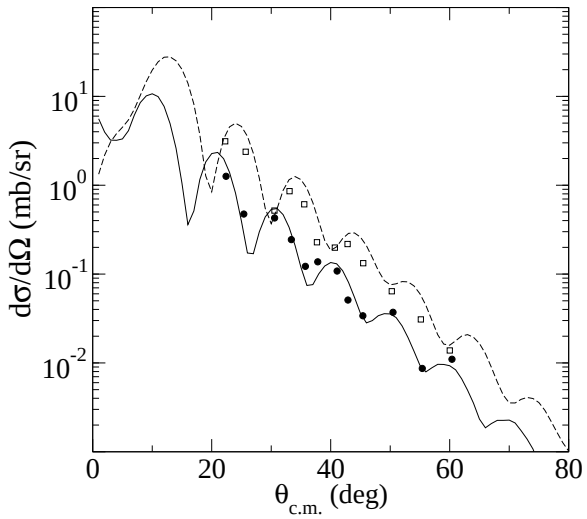

FIG. 3: Inelastic scattering to the 2_1^+ (4.08 MeV) and 3_1^- (2.61 MeV) states in ^{208}Pb. The data of Adams *et al.* for scattering to the 2_1^+ and 3_1^- states are displayed by the circles and squares, respectively. The results of the g-folding calculations made to the 2_1^+ and 3_1^- states are displayed by the solid and dashed lines, respectively.

amplitudes for inelastic scattering to the 2_1^+ and 3_1^- states in ^{208}Pb, for which the transition densities were obtained from our RPA calculation. In Fig. 3 we present results for the scattering to both the 2_1^+ and 3_1^- states. The data of Adams *et al.* to the 2_1^+ and 3_1^- states are denoted by the circles and squares respectively, while the results of the g-folding calculations made are shown by the solid and dashed lines, respectively.

As with the elastic scattering, the agreement between the results of the g-folding calculation and the data for scattering to the 2_1^+ state shown in Fig. 3 is excellent. Again, note that our calculations are predictions. In contrast, phenomenological analyses of those data [18] required a deformed spin-orbit term reflecting the density of ^{208}Pb and for which the deformation parameters for each transition were fitted to each set of data. Our result is in general agreement with that phenomenological one without the need of any additional spin-orbit components to the underlying g matrix.

In the case of scattering to the 3_1^- state (Fig. 3), the agreement between our results (predictions once more) and the data is not quite as good as those for the elastic scattering or the 2_1^+ transition. The earlier phenomenological calculation [18] does better by virtue of fitting the deformation parameters of that optical potential to the data being described. Note that both the data and our results naturally follow the phase rule of Blair [19].

It is insightful to compare our results with those of a semi-microscopic calculation [20] in which a $t\rho$ form of the optical potential with transition densities obtained from analyses of inelastic electron scattering was used. The t matrices used in that analyses were those of Love *et al.* [21]. Those analyses gave quite a good reproduction of the 3_1^- transition when the requisite densities were obtained from electron scattering data, and when just the central and two-body spin-orbit components of the t matrix were chosen. They do not, however, reproduce the 2_1^+ transition. Agreement with those data is achieved only when the central term of the t matrix is used. In part, that may be due to a problem in extracting the transition density from the available electron scattering data [20]. However, the problem may also lay in the isoscalar assumption, equating the proton and neutron densities, which

was used in constructing these optical potentials. The reason as given was that the isoscalar parts of the interaction are much larger than the isovector parts. Yet that assumption fails to conserve neutron number and so the density dependence of their potentials is not correct. This would be especially problematic in proton scattering at these energies. As proton scattering probes primarily the neutron density it is important to ensure that the correct neutron density is used. That is the case with the present calculations.

We have predicted, using a fully microscopic parameter-free model, the elastic and inelastic scattering of intermediate energy protons from ^{208}Pb. The densities used for the elastic scattering and transitions were obtained from an RPA calculation using the D1S effective NN interaction. The RPA model allowed for an effective no-core microscopic model description of the spectrum of ^{208}Pb. The skin thickness obtained using the RPA wave functions is 0.13 fm, as compared to 0.17 fm obtained from the SkM* model. Those RPA densities were folded with the Melbourne g matrices to give the microscopic optical potentials needed to describe the scattering without any fitting of parameters to the data being described *a posteriori*. Excellent agreement has been obtained for both elastic and inelastic scattering commensurate with descriptions of elastic and inelastic scattering for much lighter nuclei. As a result, we are pursuing analyses of inelastic scattering up to and including excitation of the 12^+ state. The present analyses, together with those obtained previously, constraing the skin thickness to lie in the range $0.13 < S < 0.17$ fm. While these results were obtained using the pure RPA, they give encouragement to studying the structures of heavy nuclei with nucleon scattering when one generalises also to the use of the QRPA or Generator Coordinate Method [22]. The information gained on the neutron densities of such nuclei may then be used to study effectively the neutron equation of state.

[1] B. A. Brown, Phys. Rev. Lett. **85**, 5296 (2000).

[2] S. Karataglidis, K. Amos, B. A. Brown, and P. K. Deb, Phys. Rev. C **65**, 044306 (2002).

[3] C. J. Horowitz and J. Piekarewicz, Phys. Rev. C **64**, 062802(R) (2001).

[4] Jefferson Laboratory Experiment E-00-003, spokespersons R. Michaels, P. A. Souder, and G. M. Urciuoli.

[5] B. C. Clark, L. J. Kerr, and S. Hama, Phys. Rev. C **67**, 054605 (2003).

[6] K. Amos, P. J. Dortmans, H. V. von Geramb, S. Karataglidis, and J. Raynal, Adv. in Nucl. Phys. **25**, 275 (2000), and referencees cited therein.

[7] A. Lagoyannis et al., Phys. Lett. **B518**, 27 (2001).

[8] J. Klug et al., Phys. Rev. C **67**, 031601(R) (2003).

[9] S. Karataglidis, P. G. Hansen, B. A. Brown, K. Amos, and P. J. Dortmans, Phys. Rev. Lett. **79**, 1447 (1997).

[10] R. Machleidt, K. Holinde, and C. Elster, Phys. Rep. **149**, 1 (1987).

[11] J. Raynal, *Computer program DWBA98, NEA 1209/05* (1998).

[12] J. P. Blaizot and D. Gogny, Nucl. Phys. **A284**, 429 (1977).

[13] J. F. Berger, M. Girod, and D. Gogny, Comp. Phys. Commun. **63**, 365 (1990), and references cited therein.

[14] J. Bartel, P. Quentin, M. Brack, C. Guet, and H.-B. Hakansoon, Nucl. Phys. **A386**, 79 (1982).

[15] A. Nadasen, P. Schwandt, P. P. Singh, W. W. Jacobs, A. D. Bacher, P. T. Debevec, M. D. Kaitchuck, and J. T. Meek, Phys. Rev. C **23**, 1023 (1981).

[16] W. J. Wermeer, M. T. Esat, J. A. Kuehner, R. H. Spear, A. M. Baxter, and S. Hinds, Aust. J. Phys. **37**, 123 (1984).
[17] D. Goutte et al., Phys. Rev. Lett. **45**, 1618 (1980).
[18] G. S. Adams, A. D. Bacher, G. T. Emery, W. P. Jones, D. W. Miller, W. G. Love, and F. Petrovich, Phys. Lett. **91B**, 23 (1980).
[19] K. A. Amos, I. E. McCarthy, and K. R. Greider, Nucl. Phys. **68**, 469 (1965).
[20] F. Petrovich, W. G. Love, G. S. Adams, A. D. Bacher, G. T. Emery, W. P. Jones, and D. W. Miller, Phys. Lett. **91B**, 27 (1980).
[21] W. G. Love, A. Scott, F. T. Baker, W. P. Jones, and J. D. W. Jr., Phys. Lett. **73B**, 277 (1978).
[22] P. Ring and P. Schuck, *The nuclear many-body problem* (Springer-Verlag, Berlin, 1980).